HHS Public Access

Author manuscript

Invest Radiol. Author manuscript; available in PMC 2019 December 01.

Published in final edited form as:

Invest Radiol. 2018 December ; 53(12): 742–747. doi:10.1097/RLI.0000000000000499.

Accelerated IAC screening MRI protocol with compressed sensing 3D T2-weighted sequence

Mikell Yuhasz, M.D.[1], **Michael J. Hoch, M.D.**[2], **Mari Hagiwara, M.D.**[1], **Mary Bruno, B.S**[1], **James Babb, Ph.D.**[1,3], **Esther Raithel, Ph.D.**[4], **Christoph Forman, Ph.D.**[4], **Abbas Anwar, M.D.**[5], **J. Thomas Roland Jr., M.D.**[5], and **Timothy M. Shepherd, M.D./Ph.D.**[1,3]

[1]Department of Radiology, New York University Langone School of Medicine, New York, NY

[2]Department of Radiology & Imaging Sciences, Emory University Hospital, Atlanta, GA.

[3]Center for Advanced Imaging Innovation and Research (CAI2R), New York University Langone School of Medicine, New York, NY.

[4]Siemens Healthcare GmbH, Erlangen, Germany.

[5]Department of Otolaryngology, New York University Langone School of Medicine, New York, NY.

Abstract

Background and Purpose: High-resolution T2-weighted sequences are frequently used in MRI studies to assess the cerebellopontine angle (CPA) and internal auditory canal (IAC) in sensorineural hearing loss patients, but have low yield and lengthen examinations. Because image content in the Wavelet domain is sparse, compressed sensing (CS) that uses incoherent under-sampling of *k*-space and iterative reconstruction can accelerate MRI acquisitions. We hypothesized that an accelerated CS T2 SPACE sequence would produce acceptable diagnostic quality for IAC screening protocols.

Material and Methods: 76 patients underwent 3-T MRI using conventional SPACE and a CS T2 SPACE prototype sequence for screening the IACs were identified retrospectively. Unilateral reconstructions for each sequence were separated, then placed into mixed folders for independent, blinded review by 3 neuroradiologists during 2 sessions 4^{+} weeks apart. Radiologists reported if a lesion was present. Motion and visualization of specific structures were rated using ordinal scales. McNemar, Wilcoxon, Cohen's kappa, and Mann-Whitney tests were performed for accuracy, equivalence and inter/intra-rater reliability.

Results: T2 SPACE using CS reconstruction reduced scan time by 80% to 50 seconds and provided 98.7% accuracy for IAC mass detection by 3 raters. Radiologists preferred conventional images (0.7–1.0 reduction on 5-point scale, $P < 0.001$), but rated CS SPACE acceptable. The 95% confidence for reduction in any CPA, IAC or fluid-filled inner ear structure assessment with CS SPACE did not exceed 0.5.

Corresponding Author: Timothy Shepherd, M.D./Ph.D., Department of Radiology, 2nd Floor, 660 First Ave., New York, NY 10016, timothy.shepherd@nyumc.org, Phone: 212-263-8487, Fax: 212-263-3838.

Conclusions: IAC screening MRI protocols can be performed using a 5-fold accelerated T2 SPACE sequence with compressed sensing while preserving diagnostic image quality and acceptable lesion detection rate.

Keywords

Compressed sensing; Accelerated MRI; Screening; Image quality

INTRODUCTION

Targeted MRI sequences of the internal auditory canal (IAC) are often added to MRI protocols for patients that present with sensorineural hearing loss (SNHL) or dizziness. Vestibular schwannomas are the most frequently detected lesion[1,2], yet such screening evaluations have low yield with only 3–5% revealing a detectable underlying mass or lesion[3]. Contrast-enhanced T1-weighted MRI is considered the gold-standard for diagnosing abnormalities in the cerebellopontine angle (CPA) and IAC, particularly for lesions below 2-mm in size at or near Scarpa's ganglion[4]. However, fluid-sensitive, high-resolution anatomic sequences, such as CISS or T2 SPACE, also have demonstrated >95% pooled sensitivities for the detection of masses ranging from 2–20 mm in diameter without requiring contrast administration[5–7]. Compared to CISS, T2 SPACE reduces image blurring using a fast spin echo sequence with variable flip angles, thus allowing for more accurate characterization of fine detailed structures[8]. Both fluid-sensitive, non-contrast sequences however require relatively long scan times of 4–5 minutes, thus increasing the costs and duration of IAC screening MRI examinations with low prevalence of abnormalities.

Imaging data from MRI, including the SPACE sequence, can be transformed into a sparse representation using a Wavelet transform, such that significantly less information is needed to reconstruct artifact-free images[9]. Compressed sensing (CS) is a recently described method of image reconstruction that uses incoherent sub-Nyquist k-space sampling, a transform into a sparse image representation and iterative reconstruction techniques to generate equivalent MRI exams with markedly reduced scan times[9–11]. Compressed sensing has been investigated particularly for body, pediatric and musculoskeletal imaging studies[11–18]. In neuroradiology, accelerated MRA, 2D FLAIR and T2-weighted imaging using compressed sensing compared favorably to conventional approaches[19–22]. These prior studies suggested it could be cost effective to use compressed sensing to accelerate MRI sequences or protocols used for screening of low prevalence conditions. We report the results of an initial study designed to test the hypothesis that a CS T2 SPACE sequence used as part of the IAC screening protocol would not affect diagnostic imaging quality or lesion detection rate compared to conventional imaging.

MATERIALS AND METHODS

The retrospective study was approved by the local institutional review board and compliant with the Health Insurance Portability and Accountability Act. Over two years, 76 patients (34 male, 51.2 ± 16.7 yrs) undergoing an outpatient 3-T MRI (MAGNETOM Skyra, Siemens Healthcare, Erlangen, Germany) with contrast for sensorineural hearing loss had

concurrent IAC T2 SPACE and CS SPACE prototype sequences. Since the prevalence of IAC lesions is low[3], we enriched the sample with patients followed at an otolaryngology clinic with serial MRI for relatively small IAC masses. Patients with congenital inner ear malformations, known temporal bone pathology or prior temporal bone surgery were excluded since they would not normally undergo *screening* MRI examinations at our institution. The initial enrollment goal was 75 subjects prior to initial statistical analysis. A conventional T2 SPACE was obtained of the bilateral cerebellopontine angles, IACs and fluid-filled inner ear structures with total acquisition time of 4 min 10 sec (TR/TE = 1000/134 ms, flip angle = 115º, echo train length = 65, matrix = 384 × 384, 18-cm field-of-view, slice thickness = 0.47 mm, 2 averages). The CS SPACE sequence[23], that employed variable-density Poisson disc pattern and compressed sensing reconstruction[24], was similar (TR/TE = 1000/190 ms, flip angle = 115º, echo train length = 77, matrix = 384 × 346, 18-cm field-of-view, slice thickness = 0.47 mm, 1 average), but k-space was undersampled by 75% with acquisition time of only 50 sec. Image reconstruction of the CS SPACE sequence used a regularization factor of 0.005. The undersampling and regularization chosen for the CS SPACE sequence were determined by a radiologist involved in the study during a preliminary investigation with a limited number of volunteers and based recommendations from prior literature[10] – it was not feasible to iterate through multiple CS parameter choices during an individual clinical MRI examination or ask raters to evaluate numerous image iterations per subject in such a large clinical cohort. Both sequences produced 470-micron isotropic resolution images.

The clinical report based on the interpretation of all MRI sequences by radiologists not involved in the study served as the reference standard for the presence of a lesion (20/76 subjects or 26.3%). In 56 subjects without lesions, a random side was selected for multi-planar reconstructions of the two SPACE sequences. In subjects with lesions, the affected side was always selected. The cropped field of view for reconstructions was bordered by the cerebral aqueduct posteriorly, anterior temporal horn anteriorly, pinna laterally, basilar artery medially, hypoglossal canal inferiorly and petrous ridge superiorly. Twelve subject datasets without lesions were evaluated twice by each rater to assess for intra-observer variability. Datasets with lesions were not repeated to avoid obscuring structures for repeat intra-rater assessment and to avoid the individual raters recognizing repetition of cases during the same review session. For each subject dataset, the other MRI sequences were removed, then the SPACE and CS SPACE reconstructions divided into two batches randomly such that each batch contained only one of the two sequences for an individual subject. A radiology resident not involved in rating of the individual studies organized the data.

Three blinded, board-certified radiologists with 2, 5 and 6 year’s experience then independently evaluated the individual subject SPACE data in two sessions separated by 4–6 weeks. Raters were unaware the sample had been enriched with a higher prevalence of lesions[3] or that some datasets were repeated to assess intra-rater variability. First, raters decided if a lesion was present and if so, measured its greatest dimension in the axial plane. Visualization of the edges and internal features for the cochlea, vestibule, semicircular canals, cerebellopontine angle on axial imaging, internal auditory canal (IAC) on sagittal oblique imaging (Stenver’s view), cranial nerve V in both cisternal and Meckel’s cave segments, and anterior-inferior cerebellar artery were assessed using a 5-point ordinal scale

[excellent (5), good (4), acceptable (3), poor quality (2) or unacceptable (1)]. Raters did not score structures they determined were obscured by a lesion (e.g. large schwannoma filling the IAC). Raters used the same ordinal scale for grading their subjective impression of overall image quality. Image motion degradation was evaluated using a 3-point ordinal scale [substantial motion degradation (1), mild motion (2), or no motion (3)].

Statistical Analysis:

For each rater, the SPACE and CS SPACE sequences were compared regarding lesion detection and overall accuracy for the lesion detection using McNemar tests. The greatest measured lesion axial dimension, overall subjective preference and motion ordinal scores were compared using paired-sample Wilcoxon signed-rank tests. A 95% confidence limit was determined for the upper bound of how much lower the score for CS SPACE was compared to conventional SPACE. Further, for each of these ordinal measures, an exact Mann-Whitney test was used to compare scores for individual readers for datasets where the reader detected the presence of motion or a detected lesion.

Agreement between sequences for each rater was assessed using simple kappa coefficients for lesion detection, a linear-weighted kappa for the ordinal scores and the concordance correlation coefficient for literal agreement of lesion size among lesions detected using both sequences. Agreement was considered poor when kappa (K) was <0, slight when $0 \leq K \leq 0.2$, fair when $0.2 < K \leq 0.4$, moderate when $0.4 < K \leq 0.6$ and substantial when $K > 0.6$. Subjects with lesions were not repeated in the two batches so intra-rater agreement in this subset was not assessed. For ordinal classification of image quality and motion, inter- and intra-rater agreement were characterized as the percentage of times when two raters agreed when assessing the same subject or a rater provided the same result on separate occasions respectively. Finally, the Likert scores were converted into binary outcomes with scores of 1–2 deemed unacceptable image quality and scores 3–5 deemed diagnostically acceptable image quality. The percentages of overall studies and specific structures with acceptable quality (original scores of 3–5) for conventional and CS SPACE were then compared for individual raters using a McNemar test. A 95% limit was determined for the upper bound of what percentage of studies using CS SPACE would have been deemed unacceptable compared to conventional SPACE.

RESULTS

CS SPACE acquisitions for IAC MRI screening protocols required 80% less scan time (50 seconds) compared to conventional T2 SPACE (4 minutes 10 seconds). 56 subjects had no radiologically abnormality whereas 20 subjects had masses detected on contrast-enhanced MRI (greatest axial diameter = 13 ± 7 mm; 5 lesions ≤ 5 mm, range 2.4 – 25.6 mm) (Figure 1). All masses were vestibular schwannomas by radiographic criteria, located either in the CPA or IAC, and similar in size/range to those encountered in clinical practice[25]. Using conventional T2 SPACE, all 3 independent, blinded neuroradiologists detected the 21 masses with 100% accuracy (Table 1). Using CS SPACE, 2 out of 3 neuroradiologists detected all masses, while one neuroradiologist missed a single 3-mm mass located in the IAC fundus. There were no false positives. Thus, only one decision error was made by one rater among

455 total evaluations for lesion detection (such that estimating sensitivity and specificity would be uninformative). Inter-rater agreement for lesion detection was excellent for both conventional and CS SPACE (kappa = 1.00 and 0.98 respectively). Raters also provided highly similar measurements for the maximum axial dimension of the masses (concordance correlation was ≥ 0.97 for all 3 raters) with a statistically significant 0.7 mm smaller mean measurement by rater 1 using CS SPACE (P = 0.048) not considered clinically important.

All 3 radiologists rated the overall image quality of CS SPACE as “acceptable” or better on average, however each radiologist rated overall image quality higher for conventional SPACE (P < 0.001) (Figure 2) with 95% confidence of at least a 0.5 higher mean ordinal score for each individual radiologist assessing images. All 3 raters reported observing individual examples of less motion degradation using CS SPACE (e.g. Figure 3), but this only reached significance for the assessment across all samples with rater 3 (Figure 2). Individual radiologist assessment of specific structures demonstrated similar results with small reductions in perceived quality for the CS SPACE – notably, however, the IAC appeared equivalent to all raters (Table 2). The mean rating for individual structures was 3.6 or higher in all individual assessments (between “acceptable” and “good”). The 95% confidence limit for the maximum reduction in quality by the 3 raters for CS SPACE was ≥0.3 for only 4 of the 21 comparisons (all by rater 1) and no structure had a 95% confidence limit for the difference that was >0.5. In a posthoc analysis, no significant differences were noted between studies for overall image quality or specific structure ratings between the two SPACE sequences when a lesion or motion was deemed present in an individual study.

There were small observable differences amongst raters for image assessment –e.g. rater 3, the only dedicated head and neck specialist amongst the raters, gave lower image quality scores for *both* sequences, observed significantly less motion for CS SPACE, and reported the lowest number and magnitude of statistically significant reductions in image quality for CS SPACE. The frequency of intra- and inter-rater agreement is shown in Table 3. The kappa coefficients for intra-rater agreement were fair to moderate. For inter-rater agreement, the linear-weighted kappa coefficients for overall and structure-specific quality assessment were slight or poor – it should be noted that the majority of ratings (the mode) were “4” across all quality assessments (e.g. 69.4% of all IAC ratings). Hence, agreement between two raters by chance alone would be 48% such that the kappa for inter-rater agreement would be determined as slight (0.07 and 0.15 for SPACE and CS SPACE respectively) despite agreement above 50%.

Because the emphasis was on one component sequence of an MRI screening examination, we also performed a posthoc analysis with the ratings simplified to a binary categorization as “acceptable” (rated 3–5) or “poor quality” (rated 1–2). Inter-rater agreement for overall image quality and individual structures then was high for both conventional and CS SPACE (97–100% and 92–100% respectively), but remained lower for motion (between 40.8 – 100% for both sequences and all 3 raters). The 95% upper limit for poor perceived quality studies using CS SPACE relative to conventional SPACE across raters ranged between −13.8 and 12.8%, where a 95% limit less than 0 implies that the use of CS is expected to increase the prevalence of acceptable images. Kappa is not well defined when the prevalence of acceptable images is 100% for one or both sequences, as was true for most combinations of

outcome and rater in this analysis. Rater 3 reported CS SPACE was 31% less likely to have motion degradation (P = 0.001). Otherwise, all 3 raters did not detect statistically significant differences between conventional and CS SPACE regarding “acceptable” image quality for overall preference or individual structures with agreement ranging between 94.6–100%.

DISCUSSION

Delayed detection of IAC masses in patients presenting with SNHL is associated with worse treatment outcomes and have historically contributed to ipsilateral facial nerve paralysis or hearing loss[26,27]. Currently, a contrast-enhanced T1-weighted sequence is the gold-standard for screening MRI examinations in this patient population, although multiple studies have demonstrated that non-contrast, fluid-sensitive sequences also have excellent sensitivity for IAC lesions greater than 2-mm in size[3,28–34]. This study is the first to demonstrate that a CS-accelerated SPACE sequence with an 80% reduction in required MRI scan time also can provide excellent lesion detection rate, accuracy, lesion measurement and inter-rater agreement (Table 1). There were no false positives and only 1 of 3 raters missed a single 3-mm IAC mass (1 error from 455 total evaluations) – such a small mass would normally be managed with continued observation using serial MRI, not surgical management, in a patient without other temporal bone abnormalities[35–38]. Previous studies using T2-weighted sequences also have reported that lesions 2–10 mm in size can be missed rarely by some, but not all observers[7,29,30], particularly if the lesion is smaller than the voxel dimensions[32]. Since there were 455 total evaluations, the single false negative in this CS SPACE study also may be attributed to other reasons than the MRI sequence itself[39]. The results suggest CS SPACE can provide an efficient and effective screening sequence for IAC masses in the general patient population (ideally still in conjunction with a gold-standard contrast-enhanced T1-weighted sequence). In this protocol, CS SPACE could reduce total scan time per patient by 3.3 minutes – e.g. at our local outpatient practice (with multiple additional MRI scanners besides the only one used to perform this study) approximately 75 patients undergo IAC screening MRI sequences per week, this would provide an additional 4 hours of scanner time per week (i.e. sufficient time for 8–12 additional scans in most circumstances).

Despite statistical equivalence and non-inferiority of the CS SPACE sequence for IAC mass detection, all 3 raters preferred the conventional SPACE overall (Figure 2a). Raters described CS SPACE as less inherently visually pleasing and observed visible noise in the background temporal bone (a low signal structure not normally evaluated with MRI)(Figure 1c). Previous studies show that radiologists do not like higher degrees of regularization in CS reconstructions than used here[40]. Image assessment was highly subjective and it remained hard to define as demonstrated by the relative inter-rater magnitude differences observed for either sequence on the ordinal scale. Such an incremental trade-off in image preference occurs in daily neuroradiology practice when reading studies from different field strengths, head coils or vendors without compromising diagnostic quality or reader confidence – this may be an acceptable trade-off for an IAC screening examination with only 3–5% chance of detecting a lesion[3]. Rater assessment of individual CPA and fluid-filled inner ear structures was lower for CS SPACE, but considered non-inferior (where “inferior” is defined as P-value < 0.05 and 95% confidence for maximum reduction > 0.5)

(Table 2). In this study, these were considered secondary imaging targets for SNHL screening MRI examinations, yet a small percentage of schwannomas may occur in labyrinth structures (none in this clinical cohort). Lesion detection and IAC-specific visual assessment appeared equivalent between the two SPACE sequences. When the assessment was simplified to binary classification of acceptable or unacceptable, all 3 raters did not detect statistically significant differences between conventional and CS SPACE for overall preference or individual structures with agreement ranging between 94.6–100%. Finally, rater 3 observed 31% less motion degradation ($P = 0.001$) in CS SPACE studies (Figure 2b). This likely reflects decreased macroscopic head motion occurring during the 80% reduced scan time. A motion-degraded CS SPACE sequence also could be repeated up to four times if needed without exceeding the original time required for a conventional SPACE acquisition.

There are some limitations to this study. The CS SPACE sequence was only available on a single, newer translational research 3-T MRI scanner at our institution during the study, although the results also may be applicable to other scanners, including 1.5-T MRI since SPACE is not typically a signal-limited sequence. Other causes of SNHL, such as loss of signal in the fluid-filled inner ear structures from labyrinthitis ossificans, were observed by raters in multiple subjects using both routine and CS SPACE, but were not specifically included in the analysis for 2 reasons; 1) excluding an IAC mass is the main motivation for screening MRI instead of CT in adults, and 2) this would have made data collection and statistical analysis for this initial study overly complicated. While raters were blinded and evaluated the data in batches, over the course of their evaluations they may have suspected that the prevalence of masses was much higher than the general population undergoing IAC screening MRI exams[3] introducing rate bias towards lesion detection. Enrichment also may confound the reported CS SPACE sensitivity and specificity, but it would be impractical to ask 3 raters to evaluate 400–650 cases twice (in order to reproduce a 3–5% screening SNHL MRI population prevalence[3] with 20 positive cases). Evaluations were not performed by referring otolaryngology surgeons because of the emphasis on screening. Undersampling and regularization parameters for the CS SPACE sequence were determined a priori since it would not be feasible to iterate through multiple CS parameter choices in such a large patient cohort. Similarly, the ordinal scale was chosen a priori to emphasize acceptability for diagnostic purposes – the data shows that the mean observed differences between sequences were limited to a small range centered on “good” visualization of relevant structures (Table 2). This suggests that the CS SPACE sequence is good enough that differences compared to conventional SPACE are small and hard to define objectively. A follow-up study could be designed to assess quality more discretely within this range.

There are several interesting future directions suggested by the current results. First, while this initial study demonstrated that 80%-accelerated CS SPACE in IAC screening protocols was clinically acceptable and non-inferior, alternative undersampling and regularization parameters could be explored further to find a different compromise between scan time reduction and the overall perceived quality of the images to diagnostic radiologists. CS SPACE also could be applied to other patient populations where MRI of the IAC, CPA and fluid-filled inner ear structures is obtained, such as a potential rapid exam in unsedated children with suspected inner ear malformations. Particularly for this potential population, it

also should be noted that CS reconstructions can be used conversely to increase spatial resolution for a given scan time to improve visualization of subtle structural abnormalities (e.g. 470-micron isotropic CS SPACE can be obtained of the whole head in 5 minutes). CS may be applied widely to other neuroradiology applications [15,19–22].

CONCLUSION

Compressed sensing techniques use incoherent undersampling of *k*-space and iterative image reconstruction to accelerate clinical MRI sequences because image content is sparse in the Wavelet domain. This study demonstrates that novel prototype CS techniques can be used to accelerate the T2 SPACE component of routine *screening* IAC MRI protocols by a factor of 5 while preserving adequate diagnostic image quality. While the images were slightly less satisfying overall to the evaluating radiologists, key diagnostic features were preserved and offered images potentially less susceptible to macroscopic head motion artifact.

LIST OF ABBREVIATIONS

CPA	cerebellopontine angle
CS	compressed sensing
IAC	internal auditory canal
SNHL	sensorineural hearing loss

REFERENCES

1. Kumar A, Maudelonde C, Mafee M. Unilateral sensorineural hearing loss: analysis of 200 consecutive cases. Laryngoscope. 1986;96(1):14–8. [PubMed: 3941576]
2. Armington WG, Harnsberger HR, Smoker WR, et al. Normal and diseased acoustic pathway: evaluation with MR imaging. Radiology. 1988;167(2):509–15. [PubMed: 3357963]
3. Zealley IA, Cooper RC, Clifford KM, et al. MRI screening for acoustic neuroma: a comparison of fast spin echo and contrast enhanced imaging in 1233 patients. Br J Radiol. 2000;73(867):242–7. [PubMed: 10817038]
4. Tryggvason G, Barnett A, Kim J, et al. Radiographic association of schwannomas with sensory ganglia. Otol. Neurotol. 2012;33(7):1276–1282. [PubMed: 22858714]
5. Fortnum H, O'Neill C, Taylor R, et al. The role of magnetic resonance imaging in the identification of suspected acoustic neuroma: a systematic review of clinical and cost effectiveness and natural history. Health Technol Assess. 2009;13(18):iii-iv, ix-xi, 1–154.
6. Lane JI, Ward H, Witte RJ, et al. 3-T imaging of the cochlear nerve and labyrinth in cochlear-implant candidates: 3D fast recovery fast spin-echo versus 3D constructive interference in the steady state techniques. AJNR Am J Neuroradiol. 2004;25(4):618–622. [PubMed: 15090354]
7. Abele TA, Besachio DA, Quigley EP, et al. Diagnostic accuracy of screening MR imaging using unenhanced axial CISS and coronal T2WI for detection of small internal auditory canal lesions. AJNR Am J Neuroradiol. 2014;35(12):2366–2370. [PubMed: 25034778]
8. Tong T, Yue W, Zhong Y, Zhenwei Y, Yong H, Xiaoyuan F. Comparison of contrast-enhanced SPACE and CISS in evaluating cavernous sinus invasion by pituitary macroadenomas on 3-T magnetic resonance. J Comput Assist Tomogr. 2015;39(2):222–227. [PubMed: 25526399]
9. Lustig M, Donoho D, Pauly JM. Sparse MRI: The application of compressed sensing for rapid MR imaging. Magn Reson Med. 2007;58(6):1182–1195. [PubMed: 17969013]

10. Jaspan ON, Fleysher R, Lipton ML. Compressed sensing MRI: a review of the clinical literature. Br J Radiol. 2015;88(1056):20150487. [PubMed: 26402216]
11. Vasanawala SS, Alley MT, Hargreaves BA, et al. Improved pediatric MR imaging with compressed sensing. Radiology. 2010;256(2):607–616. [PubMed: 20529991]
12. Chandarana H, Doshi AM, Shanbhogue A, et al. Three-dimensional MR cholangiopancreatography in a breath hold with sparsity-based reconstruction of highly undersampled data. Radiology. 2016;280(2):585–594. [PubMed: 26982678]
13. Chandarana H, Feng L, Block TK, et al. Free-breathing contrast-enhanced multiphase MRI of the liver using a combination of compressed sensing, parallel imaging, and golden-angle radial sampling. Invest Radiol. 2013;48(1):10–16. [PubMed: 23192165]
14. Mann LW, Higgins DM, Peters CN, et al. Accelerating MR imaging liver steatosis measurement using combined compressed sensing and parallel imaging: A quantitative evaluation. Radiology. 2016;278(1):247–256. [PubMed: 26218662]
15. Roujol S, Foppa M, Basha TA, et al. Accelerated free breathing ECG triggered contrast enhanced pulmonary vein magnetic resonance angiography using compressed sensing. J Cardiovasc Magn Reson. 2014;16(1):91. [PubMed: 25416082]
16. Zhu L, Wu X, Sun Z, et al. Compressed-sensing accelerated 3-dimensional magnetic resonance cholangiopancreatography. Invest Radiol. 2018;53(3):150–157. [PubMed: 28976478]
17. Fritz J, Raithel E, Thawait GK, Gilson W, Papp DF. Six-fold acceleration of high-spatial resolution 3D SPACE MRI of the knee through incoherent k-space undersampling and iterative reconstruction—First experience. Invest Radiol. 2016;51(6):400–409. [PubMed: 26685106]
18. Yoon JH, Lee SM, Kang H- J, et al. Clinical feasibility of 3-dimensional magnetic resonance cholangiopancreatography using compressed sensing. Invest Radiol. 2017;52(10):612–619. [PubMed: 28448309]
19. Sharma SD, Hu HH, Nayak KS. Accelerated T2*-compensated fat fraction quantification using a joint parallel imaging and compressed sensing framework. J Magn Reson Imaging. 2013;38(5): 1267–1275. [PubMed: 23390111]
20. Fushimi Y, Fujimoto K, Okada T, et al. Compressed sensing 3-dimensional time-of-flight magnetic resonance angiography for cerebral aneurysms: Optimization and evaluation. Invest Radiol. 2016;51(4):228–235. [PubMed: 26606551]
21. Yamamoto T, Fujimoto K, Okada T, et al. Time-of-flight magnetic resonance angiography with sparse undersampling and iterative reconstruction: Comparison with conventional parallel imaging for accelerated imaging. Invest Radiol. 2016;51(6):372–378. [PubMed: 26561046]
22. Yamamoto T, Okada T, Fushimi Y, et al. Magnetic resonance angiography with compressed sensing: An evaluation of moyamoya disease. PLoS ONE. 2018;13(1):e0189493–0189411. [PubMed: 29351284]
23. Li G, Zaitsev M, Büchert M, et al. Improving the robustness of 3D turbo spin echo imaging to involuntary motion. MAGMA. 2015;28(4):329–345. [PubMed: 25408109]
24. Stalder AF, Schmidt M, Quick HH, et al. Highly undersampled contrast-enhanced MRA with iterative reconstruction: Integration in a clinical setting. Magn Reson Med. 2015;74(6):1652–1660. [PubMed: 25522299]
25. Jacob A, Robinson LL, Jr, Bortman JS, et al. Nerve of origin, tumor size, hearing preservation, and facial nerve outcomes in 359 vestibular schwannoma resections at a tertiary care academic center. The Laryngoscope. 2007;117(12):2087–2092. [PubMed: 17921903]
26. van Leeuwen JP, Harhangi BS, Thewissen NP, et al. Delays in the diagnosis of acoustic neuromas. Am J Otol. 1996;17(2):321–325. [PubMed: 8723970]
27. Traquina DN, Guttenberg I, Sasaki CT. Delayed diagnosis and treatment of acoustic neuroma. The Laryngoscope. 1989;99(8 Pt 1):814–818. [PubMed: 2755290]
28. Annesley-Williams DJ, Laitt RD, Jenkins JP, et al. Magnetic resonance imaging in the investigation of sensorineural hearing loss: is contrast enhancement still necessary? J. Laryngol. Otol. 2001;115(1):14–21. [PubMed: 11233615]
29. Allen RW, Harnsberger HR, Shelton C, et al. Low-cost high-resolution fast spin-echo MR of acoustic schwannoma: an alternative to enhanced conventional spin-echo MR? AJNR Am J Neuroradiol. 199617(7):1205–1210. [PubMed: 8871700]

30. Stuckey SL, Harris AJ, Mannolini SM. Detection of acoustic schwannoma: use of constructive interference in the steady state three-dimensional MR. AJNR Am J Neuroradiol. 199617(7):1219–1225. [PubMed: 8871702]
31. Soulié D, Cordoliani YS, Vignaud J, et al. MR imaging of acoustic neuroma with high resolution fast spin echo T2-weighted sequence. Eur J Radiol. 1997;24(1):61–65. [PubMed: 9056152]
32. Hermans R, Van der Goten A, De Foer B, et al. MRI screening for acoustic neuroma without gadolinium: value of 3DFT-CISS sequence. Neuroradiology. 1997;39(8):593–598. [PubMed: 9272499]
33. Marx SV, Langman AW, Crane RC. Accuracy of fast spin echo magnetic resonance imaging in the diagnosis of vestibular schwannoma. Am J Otolaryngol. 1999;20(4):211–216. [PubMed: 10442772]
34. Naganawa S, Ito T, Fukatsu H, et al. MR imaging of the inner ear: comparison of a three-dimensional fast spin-echo sequence with use of a dedicated quadrature-surface coil with a gadolinium-enhanced spoiled gradient-recalled sequence. Radiology. 1998;208(3):679–685. [PubMed: 9722845]
35. Bakkouri WE, Kania RE, Guichard J- P, et al. Conservative management of 386 cases of unilateral vestibular schwannoma: tumor growth and consequences for treatment. Journal of Neurosurgery. 2009;110(4):662–669. [PubMed: 19099381]
36. Breivik CN, Nilsen RM, Myrseth E, et al. Conservative management or gamma knife radiosurgery for vestibular schwannoma: tumor growth, symptoms, and quality of life. Neurosurgery. 2013;73(1):48–56- discussion 56–47. [PubMed: 23417180]
37. Stangerup S- E, Caye-Thomasen P, Tos M, et al. The natural history of vestibular schwannoma. Otol. Neurotol. 2006;27(4):547–552. [PubMed: 16791048]
38. Sughrue ME, Yang I, Aranda D, et al. The natural history of untreated sporadic vestibular schwannomas: a comprehensive review of hearing outcomes. Journal of Neurosurgery. 2010;112(1):163–167. [PubMed: 19538047]
39. Lee CS, Nagy PG, Weaver SJ, et al. Cognitive and system factors contributing to diagnostic errors in radiology. AJR Am J Roentgenol. 2013;201(3):611–617. [PubMed: 23971454]
40. Li B, Li H, Kong H, et al. Compressed sensing based simultaneous black- and gray-blood carotid vessel wall MR imaging. Magn Reson Imaging. 2017;38:214–223. [PubMed: 28109887]

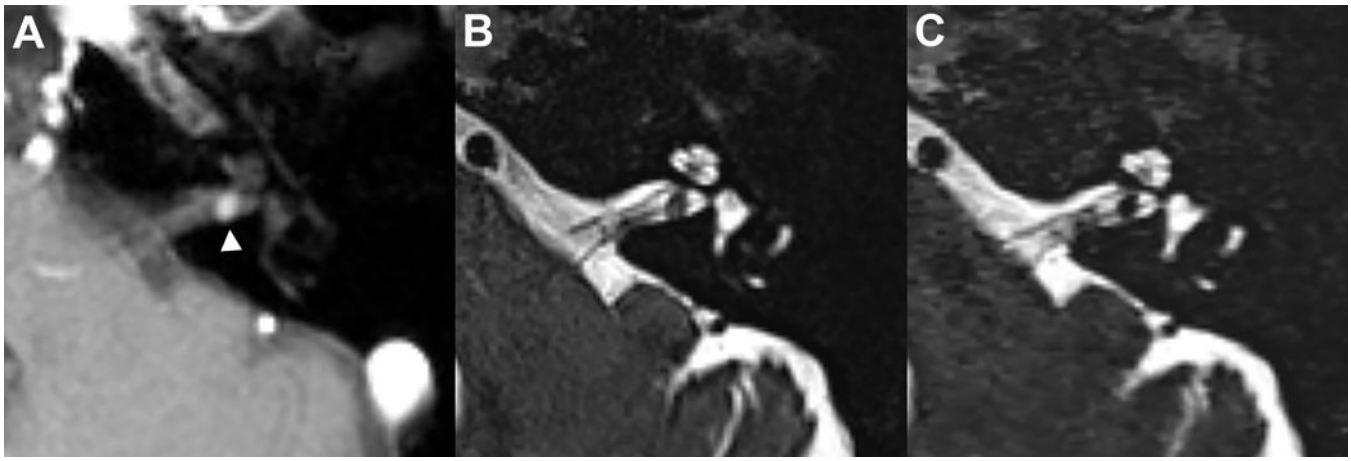

Figure 1–.

Axial post-contrast T1-weighted MRI demonstrates a 3-mm vestibular schwannoma in the posterior left internal auditory canal (A, white arrowhead). All 3 radiologists blinded to the post-contrast images independently detected this mass on the isolated companion axial conventional (B) and compressed-sensing T2 SPACE images (C)(acquisition time = 250 & 50 seconds respectively). Side-by-side comparison demonstrates more noise in the compressed sensing SPACE within the temporal bone and cerebellar parenchyma, however there is adequate detail for screening assessment of the cerebellopontine angle, internal auditory canal and fluid-filled inner ear structures.

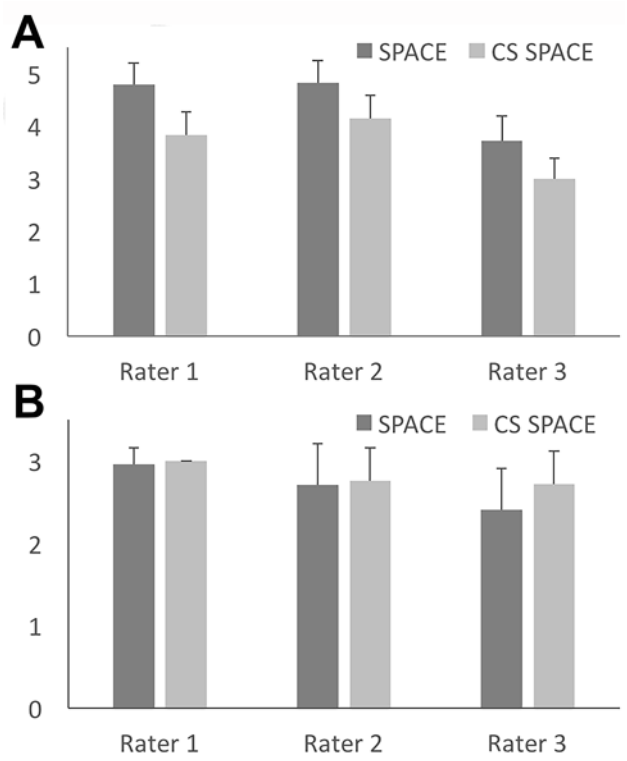

Figure 2–.

Conventional and compressed sensing SPACE images were assessed independently by 3 blinded radiologists (mean +/− SD, N= 76 per group). For subjective assessment of image quality (A), the ordinal scale was unacceptable (1), poor quality (2), acceptable (3), good (4) and excellent (5). All 3 radiologists preferred conventional SPACE ($P < 0.001$ with 95% confidence interval for rating decrease between 0.525–0.832). For the assessment of motion degradation (B), the ordinal scale was substantial motion degradation (1), mild motion (2), and no motion (3). Only rater 3 observed a significant decrease in motion degradation for CS SPACE sequences ($P = 0.048$).

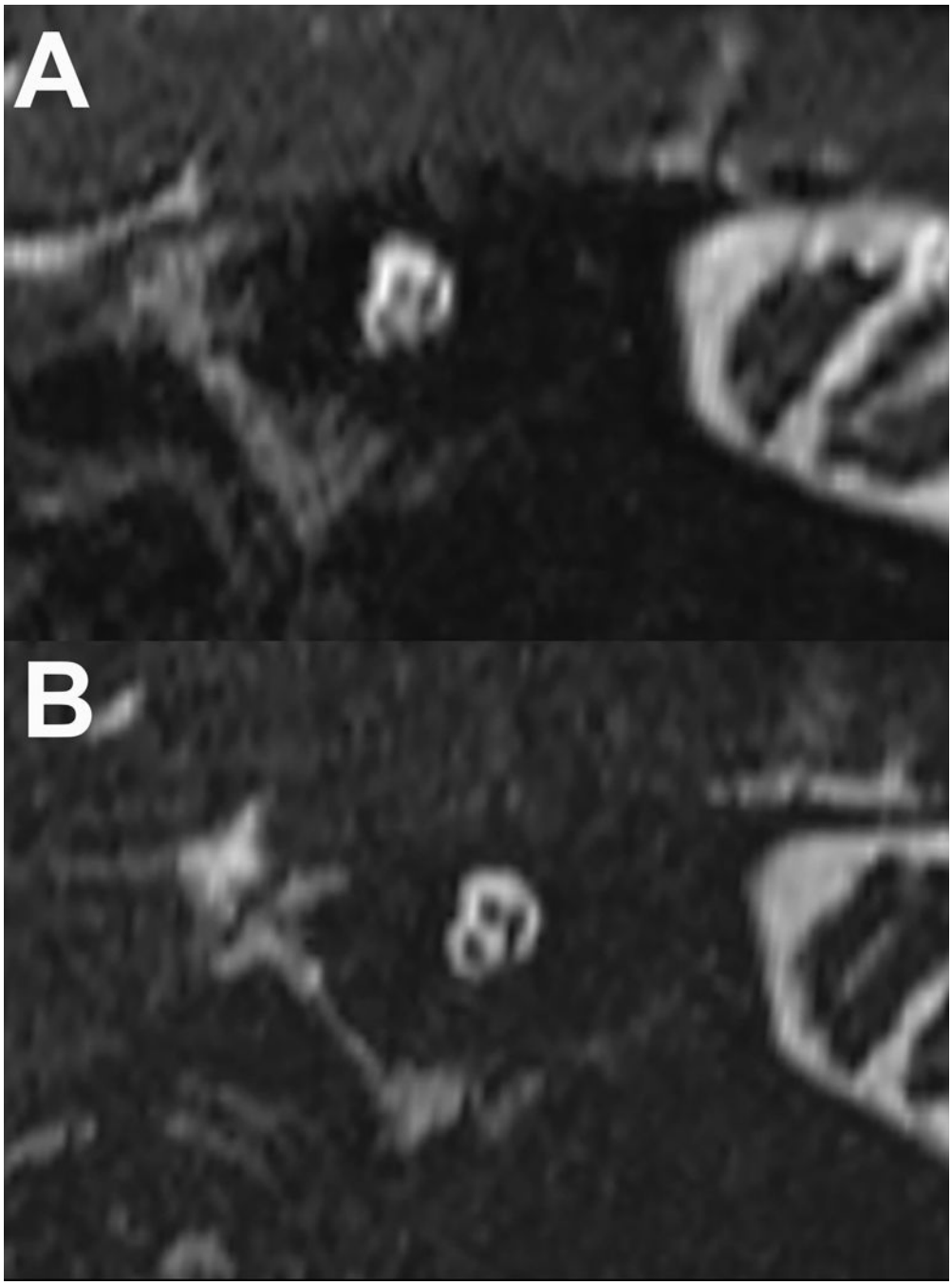

Figure 3–.

Stenver's view reconstructed image of the internal auditory canal using conventional and compressed-sensing T2 SPACE sequences (panels A & B respectively). There is less blurring at the bony margins of the IAC and less blurring of the cochlear, facial and vestibular nerves with the compressed sensing SPACE acquisition. Because this acquisition still takes 50 seconds, the motion degradation differences observed were more likely due to

decreased macroscopic head motion and not related to CSF pulsatility in the internal auditory canal.

Table 1 –

Lesion detection rate, accuracy and measurement precision for 3 independent board-certified radiologists using either conventional or compressed sensing T2 SPACE for IAC screening protocols.

Rater	Lesion detection[a]		Accuracy		Lesion size measurement (mm)[b]	
	SPACE	CS SPACE	SPACE	CS SPACE	SPACE	CS SPACE
1	26.7% (20/75)[c]	26.3% (20/76)	100% (75/75)	100% (76/76)	13.8 ± 7.6	13.1 ± 7.2[d]
2	26.3% (20/76)	26.3% (20/76)	100% (76/76)	100% (76/76)	12.9 ± 7.3	13.1 ± 7.0
3	26.3% (20/76)	25.0% (19/76)	100% (76/76)	98.7% (75/76)	13.8 ± 6.7	14.3 ± 7.4

[a] Reference standard was the postcontrast T1-weighted MRI (unavailable to radiologist raters at time of review).

[b] The maximum dimension of detected lesions in the axial plane measured by individual raters.

[c] Missing datapoint (note, there were 455 total assessments for lesion detection).

[d] P = 0.048 using paired-sample Wilcoxon signed rank test, whereas measurements from raters 2 and 3 demonstrated no difference between the two sequences.

Table 2 –

Summary of individual structure image quality assessment by 3 individual radiologists using an ordinal scale (mean ± SD, N = 76 per sequence).

Structure	Rater	SPACE	CS SPACE	P-value[a]	95% Limit[b]
AICA	1	4.9 ± 0.2	4.5 ± 0.5	< 0.001	0.251
	2	4.1 ± 0.4	4.0 ± 0.2	0.005	0.066
	3	3.9 ± 0.3	3.7 ± 0.5	0.018	0.059
CPA	1	4.9 ± 0.3	4.4 ± 0.5	< 0.001	0.349
	2	4.2 ± 0.4	4.0 ± 0.3	< 0.001	0.148
	3	3.9 ± 0.4	3.9 ± 0.4	0.675	−0.152
CNV	1	4.8 ± 0.4	4.2 ± 0.4	< 0.001	0.503
	2	4.2 ± 0.4	3.8 ± 0.4	< 0.001	0.213
	3	3.9 ± 0.2	3.5 ± 0.5	< 0.001	0.264
Cochlea	1	4.9 ± 0.3	4.4 ± 0.5	< 0.001	0.382
	2	4.2 ± 0.4	3.9 ± 0.2	< 0.001	0.158
	3	3.9 ± 0.2	3.9 ± 0.3	0.485	−0.055
IAC	1	4.2 ± 0.6	4.1 ± 0.6	0.394	−0.084
	2	3.8 ± 0.4	3.9 ± 0.4	0.732	−0.164
	3	3.6 ± 0.5	3.6 ± 0.6	1.000	−0.162
SCC	1	4.8 ± 0.6	4.4 ± 0.5	< 0.001	0.215
	2	4.1 ± 0.4	4.0 ± 0.2	0.004	0.067
	3	3.8 ± 0.4	3.9 ± 0.3	0.066	−0.243
Vestibule	1	4.9 ± 0.2	4.4 ± 0.5	< 0.001	0.436
	2	4.2 ± 0.4	4.0 ± 0.3	0.030	0.031
	3	4.0 ± 0.2	4.0 ± 0.1	0.789	−0.060

[a] Paired sample Wilcoxon signed rank test not corrected for multiple comparisons.

[b] The 95% confidence interval for the difference between individual rating of CS SPACE and SPACE (where > 0 implies SPACE would be rated better).

Table 3 –

Summary of intra- and inter-rater agreement for assessing IAC/CPA structures using conventional and CS SPACE sequences

Measure	Intra-rater agreement (N=36)		Inter-rater agreement (N=76)	
	SPACE	CS SPACE	SPACE	CS SPACE
Overall quality	69.4%	83.3%	31.0%	29.6%
Motion	66.7%	77.8%	53.5%	67.7%
AICA	91.7%	61.1%	34.9%	48.6%
CN V	77.8%	66.7%	43.7%	56.4%
CPA	100.0%	77.8%	35.1%	64.6%
Cochlea	88.9%	77.8%	35.0%	62.8%
IAC	61.1%	75.0%	51.3%	55.1%
SCC	86.1%	83.3%	35.9%	67.3%
Vestibule	91.7%	83.3%	35.8%	72.6%